Integrating Dynamic Walking and Arm Impedance Control for Cooperative Transportation

Mohamad Shafiee Motahar, Sushant Veer, Jian Huang, and Ioannis Poulakakis

***Abstract*— This paper presents a method for integrating a cooperative manipulation task in the design of dynamic walking motions for an underactuated bipedal robot. Applications that involve physical interaction between a walking biped and a leading human (or robot) collaborator, require that the biped exhibits compliance at the port of interaction with the collaborator, while at the same time be capable of adjusting its stepping pattern in response to the interaction forces developed. To achieve these objectives, the proposed method combines impedance control of the biped's arm with position control of its legs in a way that the closed-loop system adapts its stepping pattern in accordance with the collaborator's intentions. The method is applied in the case of a bipedal robot model walking over flat ground and up and down stairs of known geometry under the influence of a trajectory that is unknown to the biped and represents the intention of a collaborator.**

I. Introduction

Assistive bipedal robots must be capable of dependable locomotion in human-centric environments while simultaneously engaging in tasks that involve physical interaction with humans or other robots by means of their manipulators. In a number of such tasks – cooperative object transportation between a robot and a leading co-worker is one example – the robot's walking pattern should be adapted according to external commands, implying that the locomotion and manipulator systems *cannot* be treated in isolation. Aiming at safe cooperative manipulation and transportation, this paper focuses on combining dynamic walking with manipulator impedance control in a way that enables a bipedal robot model to be responsive to its collaborator's intentions.

A widely employed approach to regulating the dynamic interaction of a manipulator with its environment is impedance control [1], [2]. In the context of robot-human cooperation, a significant body of research focuses on adaptive or variable impedance control, with the aim of producing biomimetic behavior [3], or adapting to human characteristics and intention [4]. Impedance control is also gaining popularity in the design of prosthetic limbs that require improved performance in manipulation tasks [5], [6].

Integrating manipulation tasks within bipedal locomotion has been studied extensively in the context of humanoid robots that walk based on the zero moment point (ZMP) criterion for stability. For example, [7] presents a method which is suitable for adjusting the step length and timing of a humanoid robot in response to reference trajectories that are associated with a manipulation task; the method optimizes a cost function that combines ZMP-type stability and manipulability measures. The book [8] contains several examples of humanoids that are engaged in activities that involve their manipulators, such as pushing objects, moving obstacles out of their way, or carrying objects over a distance. However, *dynamically* walking bipeds, have not enjoyed the popularity of their quasi-static counterparts in such activities.

Various methods are available for stabilizing dynamic walking motions on bipedal robots. The hybrid zero dynamics (HZD) method [9] has been successful experimentally in generating and sustaining periodic walking motions on bipeds with point [10], as well as curved [11], feet. Other approaches involve human-inspired [12], geometric reduction [13], and stochastic control [14], methods to realize dynamic walking gaits on bipedal robots. In all these cases, however, the controllers are derived with the purpose of stabilizing locomotion alone, typically treating external forces as disturbances that need to be rejected. To the best of the authors' knowledge, only [15] investigates how manipulation tasks can be integrated with dynamic walking gaits generated using the notion of partial hybrid zero dynamics [12]. In this case, however, the control law is specifically designed so that manipulation does *not* interfere with locomotion.

Contrary to these approaches, in this paper we propose a method that enables a biped to adjust its walking pattern in response to the *interaction* forces developed as the biped's manipulator physically cooperates with a leading human (or robot) co-worker. Our motivation stems from a class of cooperative object transportation tasks, in which a bipedal robot and a collaborator interact in a way that the robot's motion is guided by the collaborator's intentions. The proposed approach combines impedance control to regulate the manipulator's motion in response to the interaction force, with position control to coordinate the actuated degrees of freedom (DOF) of the biped's legs in order to generate dynamic walking motions that can be adapted to external activity. It is deduced that, with mere knowledge of the interaction force – that is, *without* knowing the intended trajectory of the leading collaborator – the biped is capable of altering its speed as it walks on flat ground as well as up and down stairs of known geometry by changing its stride frequency while keeping its stride length constant.

II. Walking under Interaction Forces

We consider an underactuated bipedal dynamic walking model that roughly corresponds to the morphological charac-

M. S. Motahar, S. Veer and I. Poulakakis are with the Department of Mechanical Engineering, University of Delaware, Newark, DE 19716, USA; e-mail: {motahar, veer, poulakas}@udel.edu. J. Huang was with the Department of Mechanical Engineering, University of Delaware, Newark, DE 19716, USA; e-mail: jian@udel.edu.

This work is supported in part by NSF grant NRI-1327614.

teristics of the bipedal robot RABBIT [9, Table 6.3, pp 177]. The model is composed by a torso and two identical legs connected to the torso via the corresponding hip joints; see Fig. 1(a). Each leg is composed of two links, the shin and the thigh, connected through the knee joint. A two-link manipulator is attached to the torso through the shoulder joint, allowing the model to interact with its environment via external forces applied at its end effector, as shown in the schematic of Fig. 1(a). The model has seven degrees of freedom (DOF) described by the generalized coordinates $q := (q_1, .., q_7)^{\mathrm{T}} \in \mathcal{Q}$, where $\mathcal{Q}$ is a subset of $[0, 2\pi)^7$ containing physically reasonable configurations of the model. Six actuators – four located at the hip and knee joints and two at the shoulder and elbow joints – actuate the model. The toe in contact with the ground is modeled as an unactuated pin joint resulting in one degree of underactuation.

A. Interaction Model

Suppose that a leading co-worker interacts with the biped by holding the end effector of its arm with the purpose of intentionally modifying the biped's motion. An instance of this general case arises when a human and a bipedal robot cooperate to transport an object over a distance that requires the locomotion system of the robot to be engaged.

We assume that the intention of the leader can be captured by a trajectory $\mathrm{p_L}(t)$, which is selected to be a sufficiently smooth (continuously differentiable) function of time. In our approach, the biped does not have any information regarding the intention $\mathrm{p_L}(t)$ of the leader; the interaction between the biped and the leader is perceived by the biped as an external force $F_{\mathrm{e}}(t)$ applied at its end effector E. In what follows, the interaction force $F_{\mathrm{e}}(t)$ represents the only information available to the robot regarding the leader's intention.

To simulate a cooperative task such as the one described above, the intention of the leader is translated to the interaction force through an impedance model, as is common in the relevant literature [16], [17]; the purpose of this impedance model is to capture the leader's response to the robot's activity[1]. In more detail, we define the error between the location $\mathrm{p_E}(q)$ at which the end effector currently is and the location $\mathrm{p_L}(t)$ at which the leader *intends* to drive it; i.e.,

$$y_{\mathrm{L}} = h_{\mathrm{L}}(t) := \mathrm{p_L}(t) - \mathrm{p_E}(q(t)) \ . \tag{1}$$

Then, the interaction force is computed by

$$F_{\mathrm{e}} = K_{\mathrm{L}} y_{\mathrm{L}} + N_{\mathrm{L}} \dot{y}_{\mathrm{L}} \ , \tag{2}$$

where K_{L} and N_{L} are the corresponding stiffness and damping matrices; see Fig. 1(b). Note that the force $F_{\mathrm{e}}(t)$ computed by (2) is a piecewise continuous function of time.

B. Walking Model

The walking cycle consists of successive phases of single support (swing phase) and double support (impact phase).

[1]In experimental implementation, modeling the leader's impedance is not necessary; the controller only needs to know the force $F_{\mathrm{e}}(t)$, which can be provided to the biped via a force sensor.

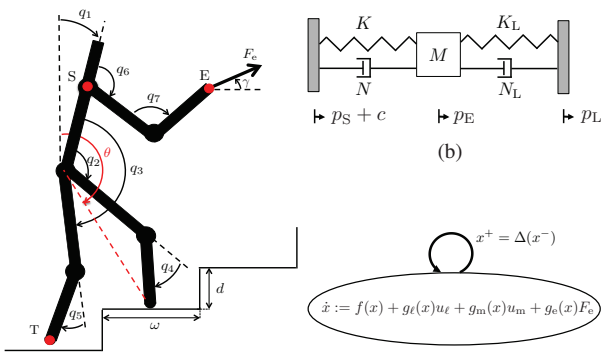

Fig. 1. (a) Robot model with generalized coordinates and stair geometry (b) Impedance model of interaction task (only horizontal component is shown). (c) Overall hybrid dynamics of the biped.

The dynamics during single support phase can be written as

$$D(q)\ddot{q} + C(q,\dot{q})\dot{q} + G(q) = B_\ell u_\ell + B_{\mathrm{m}} u_{\mathrm{m}} + J_{\mathrm{E}}^{\mathrm{T}}(q) F_{\mathrm{e}}, \tag{3}$$

where $D(q)$ is the mass matrix, and $C(q,\dot{q})\dot{q}$, $G(q)$ are vectors containing the centrifugal and Coriolis forces and the gravitational forces, respectively. The actuation distribution matrices B_ℓ and B_{m} correspond to the inputs u_ℓ and u_{m} containing the torques applied at the leg and manipulator joints, respectively. Finally, $J_{\mathrm{E}}(q) := \partial \mathrm{p_E}(q)/\partial q$, and $\mathrm{p_E}$ and F_{e} have the meaning described above; see Fig. 1(a).

Defining the state vector $x := (q^{\mathrm{T}}, \dot{q}^{\mathrm{T}})^{\mathrm{T}}$ evolving in $T\mathcal{Q} := \{x := (q^{\mathrm{T}}, \dot{q}^{\mathrm{T}})^{\mathrm{T}} \mid q \in \mathcal{Q},\ \dot{q} \in \mathbb{R}^7\}$, the swing phase dynamics can be written in state-space form as

$$\dot{x} := f(x) + g_\ell(x) u_\ell + g_{\mathrm{m}}(x) u_{\mathrm{m}} + g_{\mathrm{e}}(x) F_{\mathrm{e}} \ , \tag{4}$$

where the vector fields f, g_ℓ, g_{m}, g_{e} are defined accordingly.

The evolution of the stance phase continues until the swing leg impacts the ground in front of the stance leg. The corresponding switching surface $\mathcal{S}$ is then defined by

$$\mathcal{S} := \left\{ (q,\dot{q}) \in T\mathcal{Q} \mid \mathrm{p_T^h}(q) > 0,\ \mathrm{p_T^v}(q) = d \right\} \ , \tag{5}$$

where $\left(\mathrm{p_T^h}, \mathrm{p_T^v}\right)$ are the Cartesian coordinates of the toe of the swing leg with respect to a frame attached to the toe of the support leg, and d is the height of the stair; see Fig. 1(a).

The double support phase occurs when the swing leg contacts the ground; that is, $x \in \mathcal{S}$. As in [9, Section 3.4.2], we will assume that the double support phase is instantaneous – see [18] for accommodating double support phases with finite duration – and that the impact results in no rebound or slip. Under the assumptions of [9, HI1)-HI7), pp.50-51], the double support phase can be described by a map $\Delta : \mathcal{S} \to T\mathcal{Q}$ taking the final state $x^- \in \mathcal{S}$ of one swing phase to the initial state $x^+ \in T\mathcal{Q}$ of the next. The details on how to derive Δ are given in [9, Section 3.4.2] and are omitted for brevity. It is only mentioned that walking can be expressed as

$$\Sigma : \begin{cases} \dot{x} = f(x) + g_\ell(x) u_\ell + g_{\mathrm{m}}(x) u_{\mathrm{m}} + g_{\mathrm{e}}(x) F_{\mathrm{e}}, & x^- \notin \mathcal{S}, \\ x^+ = \Delta(x^-), & x^- \in \mathcal{S}, \end{cases}$$

where the symbols have been defined above; see Fig. 1(c) .

III. Coupled Locomotion and Arm Control

This section proposes a controller that manipulates the inputs of the arm and locomotion subsystems to ensure that the biped adapts its dynamic walking pattern to the external force. It is emphasized that the external force should *not* be interpreted as a disturbance that needs to be rejected by the arm or the locomotion system; rather, it represents a command that the system needs to follow for the successful completion of the cooperative task described in Section II.

A. Impedance Control of the Arm

The goal of the arm's controller is to establish a desired dynamical relationship between the externally applied force, $F_{\rm e}$, and the resulting motion of the arm. In particular, we are interested in the relative motion between the end effector, E, and the shoulder, S, captured by the difference of their Cartesian coordinates $\mathrm{p_E}$ and $\mathrm{p_S}$, respectively. Suppose that $\mathrm{c} \in \mathbb{R}^2$ is a constant[2] vector representing the desired location of the end effector relative to the shoulder – equivalently, the desired configuration of the arm – and define the output

$$y_{\rm m} = h_{\rm m}(q) := \big(\mathrm{p_E}(q) - \mathrm{p_S}(q)\big) - \mathrm{c} \ , \tag{6}$$

which represents the error between the actual position of the end effector with respect to the shoulder and its desired value c. Then, the objective of the controller is to impose a generalized mechanical impedance between the force applied at the end effector, $F_{\rm e}$, and the error defined by (6), so that $y_{\rm m}$ responds to $F_{\rm e}$ according to the prescription

$$M\ddot{y}_{\rm m} + \frac{N}{\epsilon}\dot{y}_{\rm m} + \frac{K}{\epsilon^2}y_{\rm m} = F_{\rm e} \ , \tag{7}$$

where $\epsilon > 0$ is a tuning parameter, and M, N, and K are positive definite mass, damping and stiffness matrices, respectively; see Fig. 1(b).

In the absence of an external force, (7) implies that the error $y_{\rm m}$ converges to zero at a rate specified by the matrices M, N, and K and the parameter ϵ, so that the arm settles at its desired configuration captured by the vector c. When $F_{\rm e} \neq 0$, the error does not converge to zero, unless the parameter ϵ in (7) is very small – in the limit, zero. In this case, the arm becomes infinitely stiff, and its joints converge rapidly to the desired configuration without being affected by the interaction force. The situation corresponds to a position controller that drives $y_{\rm m}$ to zero [19]. On the other hand, when ϵ is not small, the impedance of the arm decreases and the resulting motion is dominated by the interaction force. As a result, the parameter ϵ significantly affects the interaction between the leader and the robot; this issue will be discussed further in Section IV-C below.

To impose the desired impedance relationship (7) on the dynamics of the manipulator, a relation between the error $y_{\rm m}$ and the manipulation's input $u_{\rm m}$ is required. To achieve this, differentiate (6) twice to obtain

$$\ddot{y}_{\rm m} = \dot{J}\dot{q} + J\ddot{q} \ , \tag{8}$$

[2]In general, c can be a function of q; for example, see the Appendix where c is determined by a Beziér polynomial.

where $J := J_{\rm E} - J_{\rm S}$, and $J_{\rm E}(q) = \partial \mathrm{p_E}(q)/\partial q$ and $J_{\rm S}(q) = \partial \mathrm{p_S}(q)/\partial q$ are the corresponding Jacobians. Solving (3) for $\ddot{q}$, and substituting to (8) results in

$$\ddot{y}_{\rm m} = \dot{J}\dot{q} + JD^{-1}\Big[-C\dot{q} - G + B_\ell u_\ell + B_{\rm m}u_{\rm m} + J_{\rm E}^{\rm T}F_{\rm e}\Big] \ , \tag{9}$$

where dependence on q is suppressed. Substituting (9) to (7) and solving for $u_{\rm m}$ results in

$$u_{\rm m} = (JD^{-1}B_{\rm m})^{-1}\Big[M^{-1}(F_{\rm e} - \frac{N}{\epsilon}\dot{y}_{\rm m} - \frac{K}{\epsilon^2}y_{\rm m}) - \dot{J}\dot{q} - JD^{-1}(-C\dot{q} - G + B_\ell u_\ell + J_{\rm E}^{\rm T}F_{\rm e})\Big] \ , \tag{10}$$

where the invertibility of $JD^{-1}B_m$ requires that the arm operates away from its singular configurations. Equation (10) determines the inputs to the arm's actuators, and has the form

$$u_{\rm m} = \Gamma^{\epsilon}_{{\rm m},1}(x) + \Gamma_{{\rm m},2}(x)u_\ell + \Gamma_{{\rm m},3}(x)F_{\rm e} \ , \tag{11}$$

so that the biped's closed-loop dynamics under (11) becomes

$$\Sigma_{\rm m}: \begin{cases} \dot{x} = \bar{f}^{\epsilon}(x) + \bar{g}_\ell(x)u_\ell + \bar{g}_{\rm e}(x)F_{\rm e}, & x \notin \mathcal{S} \\ x^+ = \Delta(x^-), & x^- \in \mathcal{S}. \end{cases} \tag{12}$$

B. Locomotion Control under the Impedance Controller

The feedback controller (11) determines the inputs $u_{\rm m}$ of the arm, leaving the inputs u_ℓ of the locomotion system available for control. To realize walking motions, a control law is designed that employs u_ℓ to prescribe the motion of the actuated DOFs of the legs by driving a set of suitably selected output functions to zero. The controller is developed along the lines of [9], thus the exposition here will be terse.

To the continuous dynamics (12), we associate the output

$$y_\ell = h_\ell(q) := q_{\rm c} - h_{\rm des} \circ \theta(q) \ , \tag{13}$$

where $q_{\rm c}$ includes the controlled variables that are selected to be the relative knee and hip angles of the legs; i.e., $q_{\rm c} = (q_2, q_3, q_4, q_5)^{\rm T}$ as in Fig. 1(a). In (13), $h_{\rm des} \circ \theta(q)$ corresponds to the desired evolution of the controlled variables $q_{\rm c}$, represented as a function of the absolute angle

$$\theta(q) = q_1 + q_2 + 0.5q_4 \tag{14}$$

of the line connecting the stance leg end to the hip, as shown in Fig. 1(a). For each output, $h_{{\rm des},i}$, $i = 1, ...4$, a Beziér polynomial of degree n is selected as

$$h_{{\rm des},i}(s) = \sum_{k=0}^{n} a_{i,k}\frac{n!}{k!(n-k)!}s^k(1-s)^{n-k} \ , \tag{15}$$

where $a_{i,k}$ are the coefficients of the polynomial for each output and $s(q) = \frac{\theta(q)-\theta^+}{\theta^- - \theta^+}$ with θ^+ and θ^- being the values of $\theta(q)$ at the beginning and end of a step. It is emphasized that the virtual holonomic constraint (13) depends solely on the configuration variables associated with the locomotion system; that is, (13) depends on $q_\ell := (q_1, .., q_5)^{\rm T}$.

The objective of the controller is to drive the output (13) to zero. This can be achieved by feedback-linearizing the input/output dynamics

$$\ddot{y}_\ell = L^2_{\bar{f}^\epsilon}h_\ell(x) + L_{\bar{g}_\ell}L_{\bar{f}^\epsilon}h_\ell(x)u_\ell + L_{\bar{g}_{\rm e}}L_{\bar{f}^\epsilon}h_\ell(x)F_{\rm e} \ ,$$

where $L^2_{\bar{f}^\epsilon} h_\ell$, $L_{\bar{g}_\ell} L_{\bar{f}^\epsilon} h_\ell$ and $L_{\bar{g}_\mathrm{e}} L_{\bar{f}^\epsilon} h_\ell$ denote the Lie derivatives of h_ℓ along the corresponding vector fields of the continuous-time part of (12); see [9, Section B.1.5] for detailed definitions. Then, under the condition that the decoupling matrix $L_{\bar{g}_\ell} L_{\bar{f}^\epsilon} h_\ell$ is invertible, the control law

$$\begin{aligned} u_\ell &= \Gamma^\epsilon_\ell(x, F_\mathrm{e}) \\ &= L_{\bar{g}_\ell} L_{\bar{f}^\epsilon} h_\ell(x)^{-1} \big[v(y_\ell, \dot{y}_\ell) - L^2_{\bar{f}^\epsilon} h_\ell(x) \\ &\quad - L_{\bar{g}_\mathrm{e}} L_{\bar{f}^\epsilon} h_\ell(x) F_\mathrm{e} \big] \end{aligned} \tag{16}$$

leads to

$$\frac{d^2 y_\ell}{dt^2} = v(y_\ell, \dot{y}_\ell) \ , \tag{17}$$

and the output y_ℓ can be made to converge to zero in finite time by the controller $v(y_\ell, \dot{y}_\ell)$ used in [9, Section 5.5.1].

The system (12) under the influence of the control law (16) takes the form

$$\Sigma_\mathrm{cl} : \begin{cases} \dot{x} = f^\epsilon_\mathrm{cl}(x) + g^\epsilon_{\mathrm{e_{cl}}}(x) F_\mathrm{e}, & x \notin \mathcal{S} \\ x^+ = \Delta(x^-), & x^- \in \mathcal{S}. \end{cases} \tag{18}$$

C. Effect of Interaction Force on Locomotion

In general, the objective of the vast majority of locomotion controllers is to induce stable locomotion patterns, treating exogenous inputs as disturbances that need to be attenuated. However, the presence of persistent external forcing – as in the cooperative task of Section II – alters the nature of the task in a fundamental way: the biped needs to adapt its walking pattern to the external activity rather than trying to reject it. This section investigates how the walking controller designed in Section III-B reacts to the interaction force.

We begin our discussion with noting that under the locomotion controller of Section III-B, the interaction force F_e does not alter the stride length of the biped. Indeed, since the controller $v(y_\ell, \dot{y}_\ell)$ in (17) is selected to drive the locomotion output to zero in a finite time duration smaller than the duration of the swing phase, we have that the configuration of the legs prior to touchdown, q_ℓ^- is determined uniquely by $(h_\ell(q_\ell^-), p^\mathrm{v}_\mathrm{T}(q_\ell^-)) = (0, d)$, regardless of the configuration of the arm. In addition, since the configuration variables are not affected by the impact event, after touchdown q_ℓ^+ can be obtained by merely relabeling q_ℓ^- as in [9, HH5), pp.126], independently of the interaction force and the configuration of the arm. This discussion implies that the values θ^+ and θ^- of the angle θ at the beginning and end of the step do not change, since θ is solely a function of q_ℓ as (14) shows. As a result, the stride length of the biped remains constant over different steps, as long as the steps can be completed.

The property that the stride length cannot be changed in response to the interaction force does *not* mean that the motion of the biped remains unaffected. In fact, as will be shown in Section IV below, the biped reacts to the external force by adapting its stride frequency to accelerate or decelerate in order to catch up with the intention of the leading co-worker, as this is captured by the function $\mathrm{p_L}(t)$ in (1) and communicated to the biped via the interaction force $F_\mathrm{e}(t)$. This adaptability is essentially a consequence of the way the controller deals with the underactuated nature of the bipedal model considered. Note that there are benefits to maintaining a constant stride length, particularly in the case of walking over terrains with constrained periodic geometry. A classical example is stair traversal, where maintaining a stride length compatible stair geometry is important; see Section IV-B.

On a final note, it is worth mentioning that the arm's motion according to the impedance (7) violates hybrid invariance [9, Theorem 5.2] of the zero dynamics surface

$$\mathcal{Z} := \{ x \in TQ \mid h_\ell(q) = 0, \ L_{\bar{f}^\epsilon} h_\ell(x) = 0 \} \ ;$$

that is, $x^- \in \mathcal{Z} \cap \mathcal{S}$ does not imply that $x^+ \in \mathcal{Z}$. As a result, (18) cannot be reduced to a one degree of freedom hybrid zero dynamics (HZD) as in the case of the controllers in [9]. However, in the limit as $\epsilon \to 0$ in (7), the impedance essentially becomes equivalent to imposing an additional set of virtual holonomic constraints that correspond to the manipulator's outputs (6) being zero. Physically, this corresponds to the case of a "stiff" manipulator, that transmits the interaction force F_e to the locomotion system assuming that the arm is locked in its equilibrium configuration. In this limiting case, hybrid invariance can be recovered for an augmented zero dynamics surface $\mathcal{Z}'$, and the closed-loop system can be reduced to a single DOF analytically integrable HZD, which is driven by the external force F_e. The practical implication of this case is that explicit conditions can be stated to determine whether the biped can successfully adapt its motion to the interaction force; a brief description of this case is given in the Appendix. More details can be found in [20].

IV. Examples

In all the examples that follow, unforced periodic walking motions are computed first and then the effect of external forcing on such motions is investigated. To compute such unforced walking motions, the method of Poincaré is employed, with $\mathcal{S}$ defined by (5) being the corresponding Poincaré section. Assume that $F_\mathrm{e}(t) \equiv 0$, and let $\mathcal{A}$ be a set that includes all the parameters $\alpha \in \mathcal{A}$ introduced by the controller; namely, the constant c in (6) determining the configuration of the manipulator, and the parameters of the polynomials (15) defining the locomotion outputs (13). The Poincaré map $\mathcal{P} : \mathcal{S} \times \mathcal{A} \to \mathcal{S}$ can then be defined as

$$x[k+1] = \mathcal{P}(x[k], \alpha) \ , \tag{19}$$

and periodic walking motions can be computed by searching for fixed points $x^* \in \mathcal{S}$ and parameters $\alpha^* \in \mathcal{A}$ that satisfy

$$x^* = \mathcal{P}(x^*, \alpha^*)$$

together with additional constraints related to actuator limitations, toe-ground interaction and other specifications similar to [9, Section 3.2]. In this paper, three types of unforced periodic gaits are computed, corresponding to flat ground $(x^*_\mathrm{f}, \alpha^*_\mathrm{f})$, upstairs $(x^*_\mathrm{u}, \alpha^*_\mathrm{u})$ and downstairs $(x^*_\mathrm{d}, \alpha^*_\mathrm{d})$ walking.

The leader's intention is represented by the desired trajectories $\mathrm{p_L}(t)$ as described in Section II-A. For flat ground walking, we assume $\mathrm{p_L}(t) = (v^x_\mathrm{L} t + \mathrm{p}^x_\mathrm{E}(q(0)), \mathrm{p}^y_\mathrm{E}(q(0)))^\mathrm{T}$,

where v_{L}^x is the constant horizontal speed that the leader intends to impose and $\mathrm{p}_{\mathrm{E}}^x(q(0))$ and $\mathrm{p}_{\mathrm{E}}^y(q(0))$ are the horizontal and vertical components of the initial position of the end effector. For the stair traversal case, $\mathrm{p}_{\mathrm{L}}(t) = (v_{\mathrm{L}}^x t + \mathrm{p}_{\mathrm{E}}^x(q(0)), v_{\mathrm{L}}^y t + \mathrm{p}_{\mathrm{E}}^y(q(0)))^{\mathrm{T}}$, where v_{L}^y is the desired vertical speed of leader. Finally, to generate the interaction force F_{e}, the impedance model (2) of Section II-A is used with impedance parameters that correspond to the characteristic of human arm. Following [16], we choose $K_{\mathrm{L}} = 100\mathrm{N/m}$ and $N_{\mathrm{L}} = 20\mathrm{Ns/m}$. The impedance parameters of the biped's arm (7) are chosen to exhibit compliance in following the intended trajectory of the leader [4]; we select $K = 20\mathrm{N/m}$, $N = 4\mathrm{Ns/m}$, and $\epsilon = 1$ except in Section IV-C where ϵ varies. A video of the results accompanies the paper.

A. Adaptation to the Leader's Change of Speed

To investigate how the biped adapts to changes in the intended speed of the leader, two cases are considered. In the first case, the biped and the leader initially have the same speed until the leader suddenly accelerates; see Fig. 2(a). In accordance to (2), the interaction force shown in Fig. 2(b) increases, forcing the biped to take faster steps. When the biped reaches the intended speed, the interaction force begins to decrease, eventually causing the biped to converge to a new forced limit cycle that corresponds to the increased speed as shown in Fig. 2(c). In the second case, the leader's intended speed decreases, thereby resulting in a negative force that opposes the biped's motion; see Fig. 2(e). The biped responds to this interaction by taking slower steps, eventually matching its speed to that intended by the leader as shown in Fig. 2(d).

As was discussed in Section III-C, the stride length of the biped's walking gait remains constant as its speed changes. This can be seen in the phase portraits of the monotonic variable θ depicted in Figs. 2(c) and 2(f) corresponding to the acceleration and deceleration cases. Clearly, the range of values of θ remains the same, while the rate of change of θ changes implying that the stride frequency increases or decreases to generate faster or slower walking motions.

It is natural to ask under what conditions the biped exhibits this adaptive behavior in response to the interaction force. This question can be answered analytically in the limiting case where $\epsilon \to 0$. In short, as long as the speed of the leader is greater compared to that of the biped's unforced gait, the biped can match it on the condition that the actuator torque and friction cone limitations are not violated. On the other hand, when the leader's speed is lower than that of the unforced motion of the biped, then – in addition to the aforementioned constraints – whether the biped adapts to the leader's speed also depends on the biped's unforced gait and interaction force in a way that can be captured in analytically available expressions, as briefly discussed in the Appendix.

B. Switching from Flat Ground to Upstairs and Downstairs

The adaptability of the biped's speed to the leader's intended velocity carries to the case of walking over stairs of known geometry. However, in this case, the biped needs to be capable of switching from flat ground to upstairs or downstairs walking. To achieve this switching, the one-step transition controller described in [9, Section 7.2] is employed and the results are shown in[3] Fig. 3. Figures 3(b) and 3(e) depict the convergence of the biped's speed to the leader's intended speed for both cases of transitioning from flat

[3]In these results, the stair geometry is specified by $\omega = 20\mathrm{cm}$ and height $d = 10\mathrm{cm}$, where ω and d are depicted in Fig. 1(a).

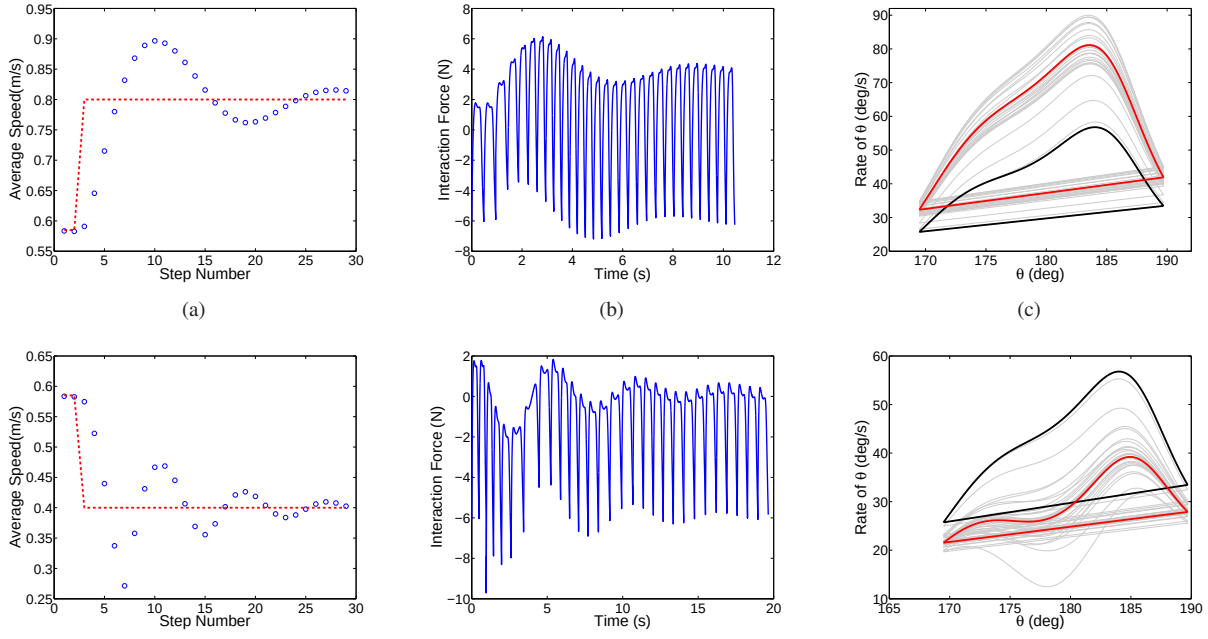

Fig. 2. **Top:** Biped response when the leader increases speed. **Bottom:** Biped response when the leader decreases speed. (a) and (d) Average speed of the leader (dashed red line) and average speed of the biped (blue marker). (b) and (e) Horizontal component of the interaction force. (c) and (f) Convergence of limit cycles. Black is the base (unforced) limit cycle, gray is the transitioning and red is the final limit cycle.

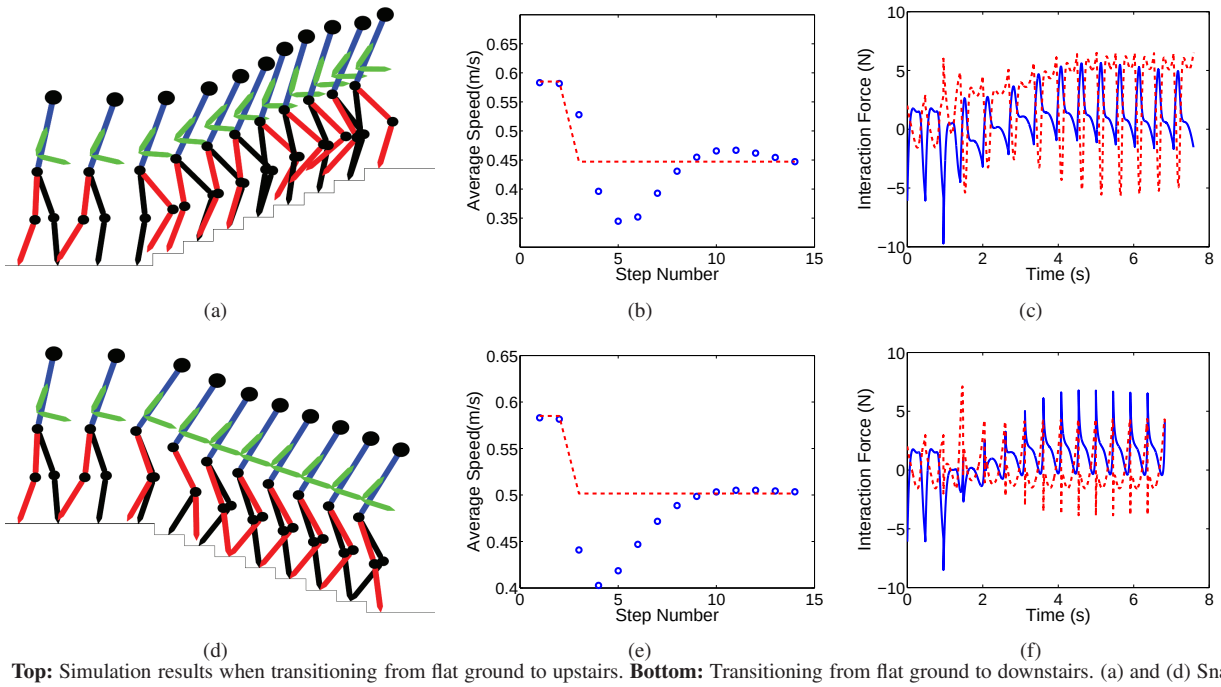

Fig. 3. **Top:** Simulation results when transitioning from flat ground to upstairs. **Bottom:** Transitioning from flat ground to downstairs. (a) and (d) Snapshots of walking. Black and red links correspond to the stance and swing foot respectively. (b) and (e) Average walking speed of the biped (blue markers) and desired speed of leader (red line). (c) and (f) Interaction force. Solid blue is the horizontal component and dashed red is the vertical component.

ground to upstairs and downstairs walking. Both components of the interaction force are plotted in Figs. 3(c) and 3(f), indicating that the leader does not need to make an excessive effort to guide the motion of the biped. As a final remark, note that the adaptation mechanism of the biped's speed – i.e., keeping the stride length constant and changing the stride frequency – is beneficial to walking over stairs with known (periodic) geometry since the biped can accelerate or decelerate while maintaining its foot placement, thereby avoiding hitting the edges of stair profile.

C. Effectiveness of the Arm's Impedance Controller

In this last section, we turn our attention to the implications of the arm's impedance controller on the magnitude of the interaction force that is developed between the biped and the leader. This force is generated by the leader, and it is desirable to keep it as small as possible to avoid excessive effort on the leader's part. To examine this issue, we focus on a scenario according to which the leader's intended speed is increased from $0.6\mathrm{m/s}$ to $0.8\mathrm{m/s}$ and different values of ϵ are used to modify the impedance (7) of the robot's arm. Figure 4 shows the root mean square (RMS) of the interaction force until the biped converges within 3% of the leader's intended speed. In interpreting this figure note that small ϵ's correspond to stiffer manipulators; in the limit $\epsilon \to 0$ the impedance controller (10) reduces to a position controller imposing the constraints (6). Clearly, stiffer manipulators result in higher interaction forces that are needed from the leader so that the biped achieves the leader's intended speed. In fact, the worst case corresponds to $\epsilon \to 0$, illustrating the benefits of impedance controllers over position controllers as in [15]. However that there is a limit on how compliant the manipulator can be, since for $\epsilon > 1.9$ the manipulator reaches its singular configuration.

V. Conclusions

This paper presented a method for integrating locomotion and manipulation tasks in a way that *dynamic* walking motions of an underactuated biped can be modified in response to the interaction forces developed at the manipulator's end effector. The proposed approach combines impedance control on the robot's arm with motion control on the robot's legs to ensure (i) compliance of the manipulator as it interacts with its environment and (ii) adaptability of the locomotion system in response to the corresponding interaction forces. It is shown that the proposed controller allows the biped to adjust its stepping pattern by altering its stride frequency, while maintaining a constant stride length – a property that is useful especially when walking over stairs is needed. The results in this paper can be used towards accomplishing cooperative object transportation tasks, in which a bipedal

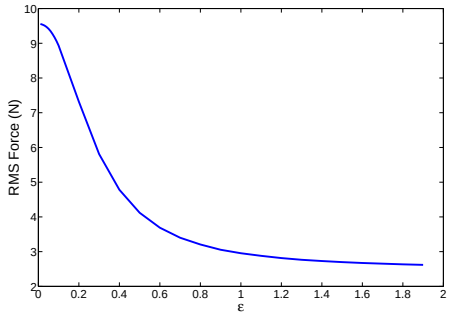

Fig. 4. RMS of the force as a function of biped impedance.

robot helps a human carry an object over a distance that engages the robot's locomotion system.

APPENDIX

In the limit $\epsilon \to 0$ the impedance controller of Section III-A reduces to imposing virtual holonomic constraints on the arm's motion [19]. In this case, by expressing the vector c in (6) as a Bézier polynomial, the zero dynamics surface

$$\begin{aligned}\mathcal{Z}' := \{x \in TQ \mid\ & h_\ell(q) = 0, L_{\bar{f}^\epsilon} h_\ell(x) = 0 \\ & h_{\mathrm{m}}(q) = 0, L_{\bar{f}^\epsilon} h_{\mathrm{m}}(x) = 0\}\end{aligned}$$

can be rendered invariant under the flow of the continuous dynamics and under the map Δ, so that the HZD

$$\Sigma_{\mathrm{z}} : \begin{cases} \dot{z} = f_{\mathrm{z}}^*(z) + g_{\mathrm{e}_{\mathrm{z}}}(z) F_{\mathrm{e}}, & z \notin \mathcal{S} \cap \mathcal{Z}' \\ z^+ = \Delta_{\mathrm{z}}(z^-), & z^- \in \mathcal{S} \cap \mathcal{Z}' \end{cases} , \quad (20)$$

is well defined. In (20), $f_{\mathrm{z}}^* := (\bar{f}^\epsilon + \bar{g}_\ell u_\ell^*)|_{\mathcal{Z}'}$ and $g_{\mathrm{e}_{\mathrm{z}}} := \bar{g}_{\mathrm{e}}|_{\mathcal{Z}'}$ are the restrictions on $\mathcal{Z}'$ of (12) in closed loop with (16), and $\Delta_{\mathrm{z}} := \Delta|_{\mathcal{S}\cap\mathcal{Z}'}$. Using the coordinate change

$$\eta = \left[h_\ell, L_{\bar{f}^\epsilon} h_\ell, h_{\mathrm{m}}, L_{\bar{f}^\epsilon} h_{\mathrm{m}}\right]^{\mathrm{T}},\ \xi_1 = \theta(q),\ \xi_2 = D_1(q)\dot{q} \quad (21)$$

where $D_1(q)$ denotes the first row of the mass matrix D in (3). In these coordinates, the HZD can be written in the form

$$\begin{aligned}\dot{\xi}_1 &= \kappa_1(\xi_1)\xi_2 \\ \dot{\xi}_2 &= \kappa_2(\xi_1) + \kappa_3(\xi_1) F_e \ ,\end{aligned}$$

in which

$$\begin{aligned}\kappa_1(\xi_1) &= \frac{\partial\theta}{\partial q} \begin{bmatrix} \frac{\partial h_\ell}{\partial q} \\ \frac{\partial h_{\mathrm{m}}}{\partial q} \\ D_1 \end{bmatrix}^{-1} \begin{bmatrix} 0 \\ 0 \\ 1 \end{bmatrix} \Bigg|_{\mathcal{Z}'} , \\ \kappa_2(\xi_1) &= -\,G_1|_{\mathcal{Z}'} \ , \\ \kappa_3(\xi_1) &= J_1^{\mathrm{T}}|_{\mathcal{Z}'} \ ,\end{aligned}$$

where G_1 and J_1^{T} are the first rows of G and $J_{\mathrm{E}}^{\mathrm{T}}$ respectively. The discrete part of Σ_{z} in (20) takes the form $\Delta_{\mathrm{z}}(z^-) = [\theta^+ \ \ \delta_{\mathrm{z}}\xi_2^-]^{\mathrm{T}}$ where δ_{z} is a constant that can be computed as in [9, Section 5.4.1, pp.128]. Then, the HZD can be integrated analytically over a step to result in the step map. Analyzing the domain of definition of the resulting step map gives the following sufficient condition for the biped to take a well defined step under the influence of a bounded external force:

$$\frac{1}{2}(\xi_2^*)^2 \geq \frac{1}{1-\delta_{\mathrm{z}}^2}\tilde{W}(\theta^-) + \frac{1}{\delta_{\mathrm{z}}^2} M \ , \quad (22)$$

where

$$\begin{aligned}\tilde{W}(\xi_1) &= F \int_{\theta^+}^{\xi_1} \frac{1}{\kappa_1(\xi)} \kappa_3(\xi)\hat{r}(\xi) d\xi \ , \\ M &= \max_{\theta^+ \leq \xi_1 \leq \theta^-} \left[V(\xi_1) + \tilde{W}(\xi_1) \right] \ , \\ V(\xi_1) &= -\int_{\theta^+}^{\xi_1} \frac{\kappa_2(\xi)}{\kappa_1(\xi)} d\xi \ ,\end{aligned}$$

and ξ_2^* is the value of ξ_2 at an unforced periodic gait, $F = \sup_t \|F_{\mathrm{e}}(t)\|_2$ and $\hat{\mathrm{r}}(\xi_1)$ is the unit vector along the direction defined by κ_3. Conditions like (22) explicitly couple information about the external force with the motion of the biped and are easily computable, but only when $\epsilon \to 0$.

REFERENCES

[1] N. Hogan, "Impedance control: An approach to manipulation: Part III - Applications," *Journal of dynamic systems, measurement, and control*, vol. 107, no. 2, p. 17, 1985.

[2] R. Kelly, R. Carelli, M. Amestegui, and R. Ortega, "On adaptive impedance control of robot manipulators," in *Proceedings of IEEE International Conference on Robotics and Automation*, 1989, pp. 572–577.

[3] G. Ganesh, A. Albu-Schaffer, M. Haruno, M. Kawato, and E. Burdet, "Biomimetic motor behavior for simultaneous adaptation of force, impedance and trajectory in interaction tasks," in *Proceedings of IEEE International Conference on Robotics and Automation (ICRA)*, 2010, pp. 2705–2711.

[4] E. Gribovskaya, A. Kheddar, and A. Billard, "Motion learning and adaptive impedance for robot control during physical interaction with humans," in *IEEE International Conference on Robotics and Automation (ICRA)*, 2011, pp. 4326–4332.

[5] A. Blank, A. M. Okamura, and L. L. Whitcomb, "Task-dependent impedance improves user performance with a virtual prosthetic arm," in *Proceedings of IEEE International Conference on Robotics and Automation (ICRA)*, 2011, pp. 2235–2242.

[6] J. W. Sensinger and R. Weir, "User-modulated impedance control of a prosthetic elbow in unconstrained, perturbed motion," *IEEE Transactions on Biomedical Engineering*, vol. 55, no. 3, pp. 1043–1055, 2008.

[7] K. Inoue, H. Yoshida, T. Arai, and Y. Mae, "Mobile manipulation of humanoids-real-time control based on manipulability and stability," in *Proceedings of IEEE International Conference on Robotics and Automation*, vol. 3, 2000, pp. 2217–2222.

[8] K. Harada, E. Yoshida, and K. Yokoi, Eds., *Motion Planning for Humanoid Robots*. Springer-Verlag, 2010.

[9] E. R. Westervelt, J. W. Grizzle, C. Chevallereau, J. H. Choi, and B. Morris, *Feedback Control of Dynamic Bipedal Robot Locomotion*. Boca Raton, FL: CRC Press, 2007.

[10] K. Sreenath, H. Park, I. Poulakakis, and J. Grizzle, "A compliant hybrid zero dynamics controller for stable, efficient and fast bipedal walking on MABEL," *International Journal of Robotics Research*, vol. 30, no. 9, pp. 1170–1193, 2011.

[11] A. E. Martin, D. C. Post, and J. P. Schmiedeler, "The effects of foot geometric properties on the gait of planar bipeds walking under hzd-based control," *International Journal of Robotics Research*, vol. 33, no. 12, pp. 1530–1543, 2014.

[12] A. D. Ames, "Human-inspired control of bipedal walking robots," *IEEE Transactions on Automatic Control*, vol. 59, no. 5, pp. 1115–1130, May 2014.

[13] R. Gregg and M. Spong, "Reduction-based control of three-dimensional bipedal walking robots," *International Journal of Robotics Research*, vol. 29, no. 6, pp. 680–702, 2009.

[14] C. O. Saglam and K. Byl, "Robust policies via meshing for metastable rough terrain walking," in *Robotics: Science and Systems*, 2014.

[15] A. D. Ames and M. Powell, "Towards the unification of locomotion and manipulation through control lyapunov functions and quadratic programs," in *Control of Cyber-Physical Systems, Lecture Notes in Control and Information Sciences*. Springer, 2013, pp. 219–240.

[16] F. Popescu, J. M. Hidler, and W. Z. Rymer, "Elbow impedance during goal-directed movements," *Experimental brain research*, vol. 152, no. 1, pp. 17–28, 2003.

[17] M. M. Rahman, R. Ikeura, and K. Mizutani, "Investigation of the impedance characteristic of human arm for development of robots to cooperate with humans." *JSME International Journal Series C*, vol. 45, no. 2, pp. 510–518, 2002.

[18] K. A. Hamed, N. Sadati, W. A. Gruver, and G. A. Dumont, "Stabilization of periodic orbits for planar walking with noninstantaneous double-support phase," *IEEE Transactions on Systems, Man and Cybernetics - Part A: Systems and Humans*, vol. 42, no. 3, pp. 685–706, May 2012.

[19] N. H. McClamroch, "A singular perturbation approach to modeling and control of manipulators constrained by a stiff environment," in *Proceedings of the IEEE Conference on Decision and Control*, Tampa, Florida, December 1989, pp. 2407–2411.

[20] S. Veer, M. S. Motahar, and I. Poulakakis, "On the adaptation of dynamic walking to persistent external forcing using hybrid zero dynamics control," in *Proceedings of IEEE International Conference on Intelligent Robots and Systems (IROS)*, Hamburg, Germany, September/October 2015.